Proceedings of the 1st Global Power and Propulsion Forum
GPPF 2017
Jan 16-18, 2014, Zurich, Switzerland
www.pps.global

GPPF-2017-166

APPLICATION OF AN INTEGRALLY GEARED COMPANDER TO AN SCO2 RECOMPRESSION BRAYTON CYCLE

Jason Wilkes, Ph.D.
Jeffrey Bennett
Joshua Schmitt

Southwest Research Institute
San Antonio, TX, USA

Karl Wygant, Ph.D.
Rob Pelton

Hanwha Techwin
Houston, TX, USA

ABSTRACT

Integrally geared (IG) compressors, expanders, and companders (combination of expansion and compression stages) are widely used in both air and process gas industries, where the technology has been proven to be reliable and provide increased overall machinery efficiency as compared to barrel-type compressors. The current work describes a novel power block concept for use in a supercritical CO_2 (sCO_2) recompression cycle for concentrating solar power applications. This concept features an integrally-geared compressor-expander, or IG compander (IGC), that allows for reduced cost by utilizing a low-cost, low-speed generator to drive high speed pinions. In addition, each pinion may operate at different rotational speeds to optimize performance, and easily allow for inter-stage cooling and expander reheating to further enhance both stage and cycle efficiency. An IGC offers compact packaging that can be easily customized for site specific needs.

Because of the close integration of all turbomachinery elements into a single machine, the IGC design optimally lends itself to power block modularization, which makes it suitable for waste heat recovery, fossil fuel power plants, and especially CSP applications. In addition, some range-extension and process control features are more easily implemented in IG compressors and expanders due to their unique and accessible geometry compared to beam style turbomachinery. This includes features such as inlet guide vanes (IGVs), variable-geometry diffuser vanes, and variable-geometry expander nozzles. Application of these geometries yields solutions to some of the challenges associated with heat input variation and compressor range requirements in CSP applications due to varying solar irradiance, temperature, and power demand. The current work describes the cycle, application, and the optimization of the cycle and plant to maximize efficiency and minimize LCOE.

INTRODUCTION

The primary motivation driving cycle innovation for CSP applications is to realize further reduce the cost of renewable power to be more competitive with traditional fossil fuel plants. The National Renewable Energy Laboratory (NREL) has published extensive assessments of the levelized cost of electricity (LCOE) of CSP installations. NREL, in cooperation with Sandia National Laboratories, developed a System Advisor Model (SAM), a renewable energy plant cost model simulator [1]. In an early study NREL modeled both parabolic trough and power tower CSP systems using Daggett California as a reference location for a CSP plant. The authors predicted that the LCOE of a molten salt power tower with a conventional steam Rankine cycle could reach 9.4 ¢/kWh.

To accelerate the advancement of solar technologies, the U.S. Department of Energy funded the SunShot initiative. NREL published the SunShot Vision Study in 2012, providing more aggressive targets for improving the cost of solar power. The Vision Study suggested that by 2020, the LCOE of a solar power tower could be as low as 6¢/kWh [2]. The study provided targets for key power tower technologies, the solar field, receiver, thermal storage, and power block. Funding was awarded for development of each of these technologies. The Vision Study postulated that achieving a power block with costs as low as \$900/kW would require an innovative sCO_2 cycle.

Closed loop sCO_2 power cycles offer high-energy conversion efficiencies as demonstrated through thermodynamic cycle models. Cycle models offer an efficient means to evaluate a variety of cycle configurations across changing environmental conditions and power demands. The present work builds upon the literature by using established sCO_2 cycle modeling assumptions, and fluid properties from NIST REFPROP.

As established in [3] and [4], the current analysis assumes that optimum recompression cycle performance occurs when the temperature of combining flow streams matches. The present work builds upon this approach by also assuming that the pressure of combined flow streams must be equal. If there is a mismatch in temperature or pressure of combining flow streams, then entropy will be generated and energy lost.

Due to the large variations in heat capacity around the critical point, the present work follows the precedent of [5] by determining heat exchanger performance using enthalpy balances. The more common approach is the

Effectiveness-NTU method [6] that uses the minimum heat capacity, which can provide inaccurate results due to the aforementioned variations in the fluid heat capacity.

The present work improves upon previous sCO_2 power cycle modeling by including pressure drops occurring in heat exchangers, generator losses, and turbomachinery mechanical losses. Target pressure drops in heat exchangers for concentrated solar power applications are in the range of 1-3% [7], which, depending on the application, may be enough to deter against a second or third stage of inter-heating. Generator losses and turbomachinery mechanical losses can also be significant. By including heat exchanger pressure drops, generator losses and turbomachinery mechanical losses; the present work strives to provide a more complete picture of achievable sCO_2 power cycle efficiencies.

Some of these improvements are noted in preliminary work detailed by Wilkes et al. [8]; however, the current work expands upon the literature by including off-design cycle and plant performance as a function of compressor inlet temperature. The off-design performance was maximized by implementing a genetic algorithm to determine the best combination of IGV angle, inventory control pressures, and design point temperature. This performance was then integrated into the SAM model to determine how the off-design performance had an impact on LCOE.

CYCLE OPTIMIZATION

The basic details of the cycle development follow the procedure given in [8] with minor improvements and introduce the impact of off-design operation on cycle and plant performance. The objective of the optimization process was to achieve the best possible efficiency within the performance and mechanical constraints of using an IGC as the power block. The target for this optimization as specified in the APOLLO FOA was 50%. Initially, the cycle calculations focused on design point estimations of cycle efficiency, and these results will be presented first, as they drive off-design cycle performance. For this analysis, the power block efficiency is defined as the ratio of the work output through the generator, as electricity, to the heat added to the cycle; thus, it accounts for turbomachinery, recuperator, and generator efficiencies, as well as pressure losses in heat exchangers.

Cycle modeling was performed using Numerical Propulsion System Simulation (NPSS) [9], an established thermodynamic tool commonly used in the air breathing engine industry. NPSS was selected for its ability to quickly perform system design parameter sweeps. NPSS was linked to National Institute of Standards and Technology (NIST) Reference Fluid Properties (REFPROP) [11] to provide accurate fluid properties of CO_2. As established in the literature, notably [4] and [5], recompression cycle designs are often constrained such that the temperature must match when flow streams recombine. Additionally, cycle models were constrained such that the combination of flow streams occurred at equal pressures to prevent losses. To verify the NPSS cycle modeling approach, a comparison was performed with the recompression cycle with intermediate re-heat used in [4], and it was found that the predicted cycle efficiencies matched within 0.04%.

The wide-range integrally-geared (WRIG) Compander project focuses on the design of unique turbomachinery; however, there are many other components to consider when modeling an sCO_2 cycle. Therefore, a literature review was conducted to find realistic pressure limitations for state-of-the-art heat exchangers, recuperators, and piping. Another constraint was the decision to keep the CO_2 in the supercritical region throughout the recompression cycle. The results of the literature review were combined with aggressive turbomachinery efficiency targets to determine appropriate model inputs that have been summarized in Table 1. While this research constrained many facets of the cycle, a number of design choices remained, including (1) the use of intercooling and/or inter-heating, (2) the selection of cycle pressure ratio, and (3) the percentage of flow split between the main compressor and re-compressor.

Table 1: Cycle Model Inputs

Group	Property	Value
Heat Exchanger	Pressure Drop (each Heat Exchanger)	1 %
	High Temp Recuperator Effectiveness	97 %
	Minimum Pinch Temperature	5 °C
	Heater Outlet Temperature	705 °C
	Cooler Outlet Temperature Range	35-55°C
Generator and Mechanical Efficiencies	Generator Efficiency	98.7%
	Compressor Mechanical/Pinion Losses	4%
	Turbine Mechanical/Pinion Losses	2%
Pressure Limits	System Min Pressure	1,070 psia
	System Max Pressure	3,953 psia
Turbomachinery	Compressor Isentropic Efficiency	83.5%
	Re-Compressor Isentropic Efficiency	84%
	Turbine Isentropic Efficiency	92%

The WRIG compander design is unique in that the two main compressor stages and four turbine stages are physically separated from one another, thus, intercooling and inter-heating is more natural to incorporate into the design. A schematic of the cycle with all possible re-heat and intercooling stages is shown in Figure 1. To determine which configurations of intercooling and inter-heating would be most advantageous, eight cycle configurations were simulated across a variety of flow splits and pressure ratios for a constant compressor inlet temperature. Another factor considered for the intercooling scenarios was the amount of compression handled by the first and second stages. The best efficiencies of this study as a function of pressure ratio are shown in Figure 2.

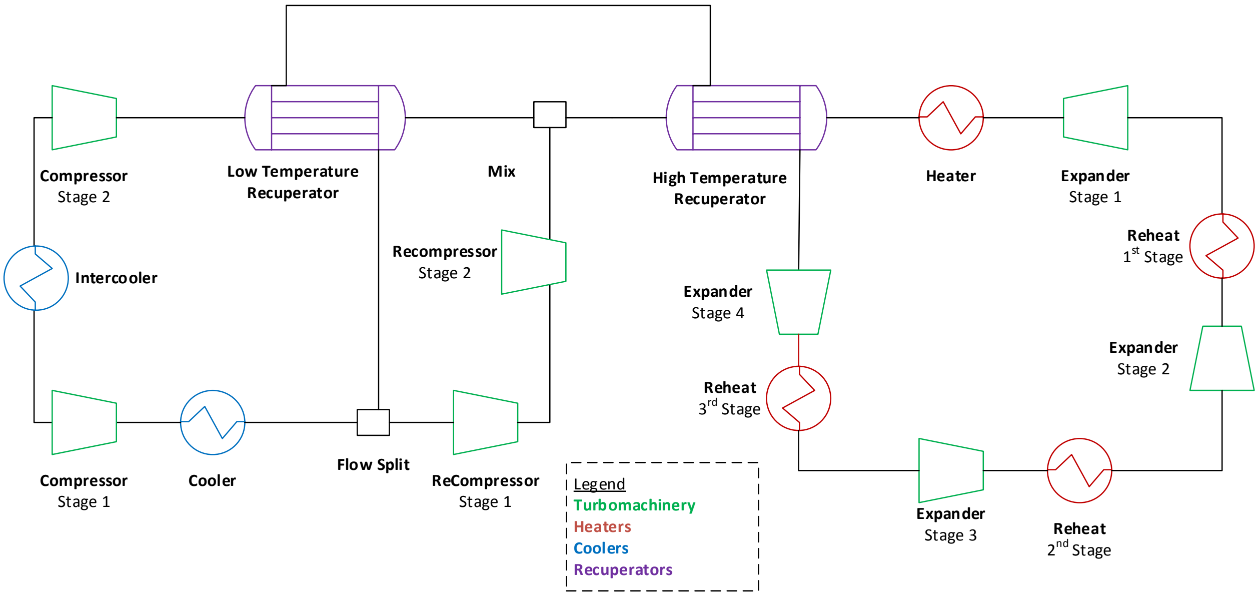

Figure 1: Cycle Schematic Shown with all possible Intercooling and Inter-heating Options

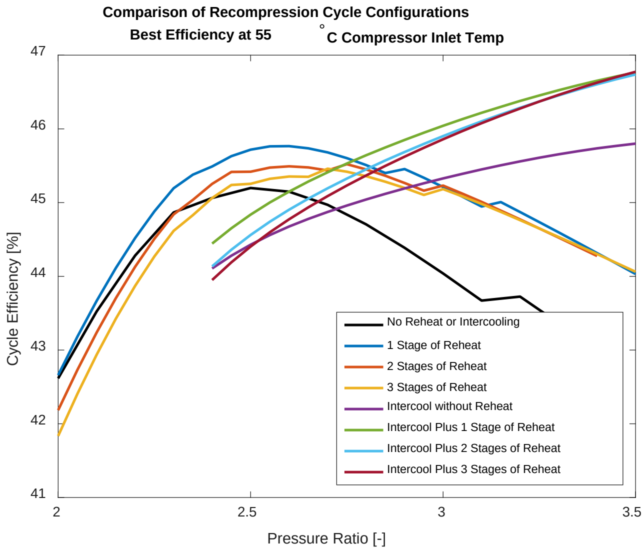

Figure 2: Comparison of Re-heat/Intercool Options at 55°C Inlet Temperature

The results show two groups of curves. The first group, denoted by efficiencies peaking near a pressure ratio of 2.5, do not have intercooling. The best efficiency in this group is the configuration with one stage of re-heat that is located between the second and third expansion stages. Additional stages of re-heat may increase the power output of the cycle, but due to the additional pressure losses caused by including more heat exchangers, the cycle efficiency does not benefit. The second group that is noted by efficiencies increasing up to a pressure ratio of 3.5, which was the limit of this study, has compressor intercooling. With increased piping strengths, there may be additional realizable configurations with intercooling above pressure ratios of 3.5; however, these were not considered in this study. Similar to the first group, one stage of re-heat offers the highest efficiency, on the order of 0.5% to 1% gain relative to configurations that do not have turbine reheating.

The previous study found two distinct cycle configurations that had promising efficiencies, a single stage of turbine reheat between the second and third stage with and without intercooling. These configurations were optimized at various inlet temperatures to determine the best efficiency point for the cycle as a function of compressor inlet temperature, pressure ratio, and flow split. The best efficiency points for each compressor inlet temperature are shown in Figure 3. As expected, lower compressor inlet temperatures correspond with generally higher cycle efficiencies. These results show that an efficiency of 50% is achievable for the configuration with one stage of re-heat with and without intercooling at 36.5°C and 39.6°C, respectively. These temperatures are near the average temperature expected at the inlet of the compressor throughout the year based on a 15°C temperature rise from ambient; therefore, it seems to be a reasonable choice for the cycle design point. At higher compressor inlet temperatures, intercooling has the advantage, while at lower temperatures it does not. The flow split for intercooling remains close to 32% mass flow to the recompressor while the configuration without intercooling diverts increasingly more flow to the recompressor as the compressor inlet temperature decreases.

Figure 3 shows the challenge in maintaining optimal cycle efficiencies as the inlet temperature to the compressor varies. Consider operating in the afternoon with an inlet temperature of 50°C (denoted by point A on the figures). At this time, running with a pressure ratio of 3.5 with compressor intercooling and one stage of re-heat provides the best efficiency. As the temperature of the ambient air decreases, eventually settling at a compressor temperature of 40°C, the plant will have to switch from the compressor intercooling to a configuration without intercooling at a pressure ratio of 3 to maintain maximum cycle efficiency. Note that this simplification is assuming that the component machinery efficiency is still operating at design. This configuration would result in less dense gas at the inlet of the compressor and recompressor. Additionally, the ideal flow split shifted from 32% to 28%, further increasing the compressor actual flow. This scenario shows the challenge of maintaining high compressor efficiency with changing ambient air temperature.

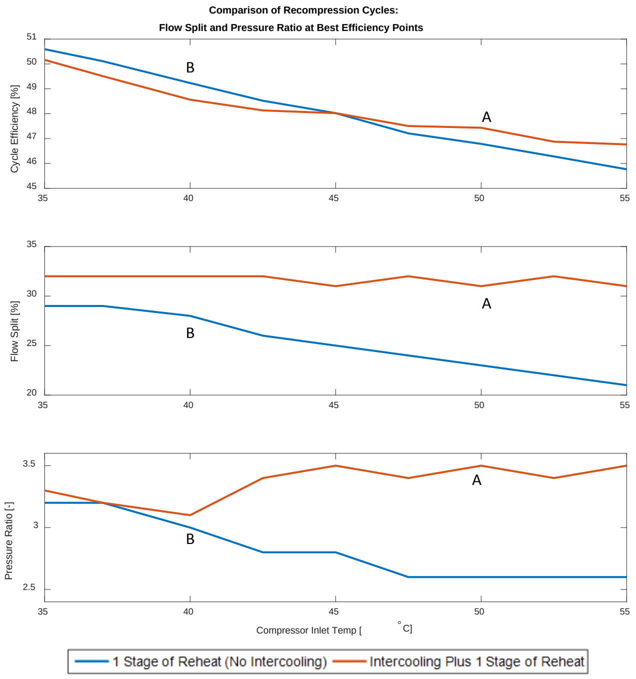

Figure 3: Flow Split and Pressure Ratio of Maximum Efficiency Point against Compressor Inlet Temperature

To better answer these questions, the authors performed off-design cycle analysis to investigate the impact of inlet guide vane angle, inventory control, compressor design point temperature on cycle efficiency. For off-design predictions, the operation of each turbomachinery stage was predicted using a map of efficiency and head versus volumetric flowrate, and the operation of each recuperator was estimated by scaling the heat transfer and pressure drop based on changes in flow conditions. A genetic algorithm was implemented to optimize the cycle performance for each compressor design for every operating temperature. Based on ambient conditions, it is expected that the compressor inlet temperature will vary between 32°C and 55°C. Therefore, off-design predictions have been focused on comparing operation in this temperature range.

Off-design predictions focused on two comparisons. The first comparison was of two cycles (one having "Intercool + Reheat," and the other "Reheat Only") having a design point compressor inlet temperature of 35°C. Predicted cycle efficiencies versus temperature for these two cases are shown in Figure 5. Note that the "Reheat Only" produces a higher efficiency throughout the range of compressor inlet temperatures investigated. This notion was presented for cooler compressor inlet temperatures while investigating on-design operation; however, this comparison confirms that "Reheat Only" is the appropriate cycle configuration for this application when considering the temperature range of typical off-design operation.

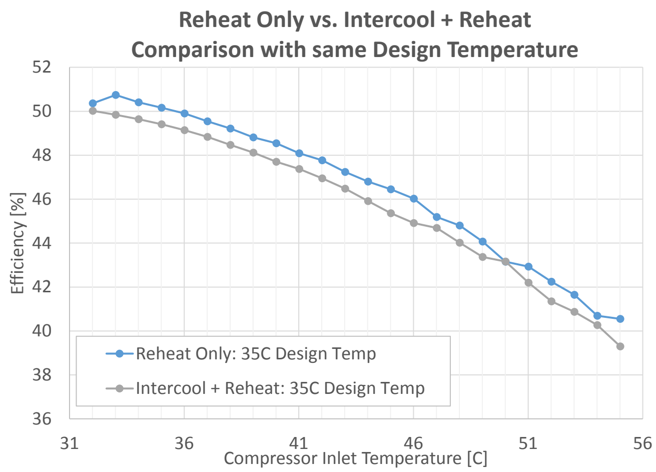

Figure 4: Comparison of Reheat Only and Intercooling + Reheat at 35°C

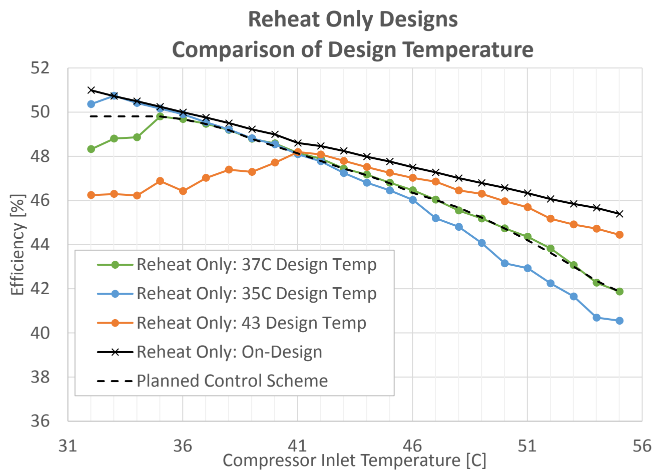

Figure 5: Comparison of "Reheat Only" Cases at 35°C, 37°C, and 43°C

The second comparison that was performed was for three cycles each with one stage of reheat and no intercooling ("Reheat Only") having different design point compressor inlet temperatures. The three designs were for compressor inlet temperatures of 35°C, 37°C and 43°C. Figure 5 compares the results of these designs. Each cycle performs best within 2°C of its design temperature, with cycle efficiencies that decrease outside of this range in either direction. Note that the 43°C design temperature performs better than the other cycles at high temperatures, while the 35°C design temperature performs better when it is cooler; therefore, it is necessary to determine where the cycle will operate most often in order to determine which design temperature is best for this particular application. For the current application using the SunShot vision study (SVS) sight, the average compressor inlet temperature throughout the year is expected to be 37°C. This temperature has been selected as the best balance between efficiency at the design temperature and at off-design. Performing a rigorous investigation of this selection requires that this project's system advisor model (SAM) be coupled to the temperature dependent efficiency and power of the cycle model; however, as will be discussed in a later section, the current version of SAM does not allow for this input. This comparison shows that a design temperature of 37°C reaches a maximum efficiency of 49.8% (within margin of error for 50% goal) and produces higher efficiencies than the 35°C design at higher temperatures; therefore, this temperature was selected be the design point for the current program.

Further investigation into the optimal operating points found for the 37°C design indicated that some non-smooth variation in control parameters would be required to achieve these points. Thus, an initial control scheme was developed that would be more practical to implement. This was done by smoothing the temperature-dependent optimized variables with fitted functions. The predicted efficiencies for this scheme are nearly identical to the optimal efficiencies and are shown in Figure 5 as "Planned Control Scheme." When reviewing the results on turbomachinery maps, the general trend is for the volumetric flowrate to increase through the compressor stages as the compressor inlet temperature increases and for it to decrease through the turbine stages.

OPTIMIZING THE SYSTEM ADVISOR MODEL (SAM)

The stated goal of the recent APOLLO funding opportunity announcement (FOA) [15] is to develop solar technologies that compete with baseload energy rates, i.e., a levelized cost of electricity (LCOE) of 6 cents per kilowatt-hour or less. To accomplish this, the FOA requires that the LCOE be justified with the SAM software developed by the National Renewable Energy Laboratory (NREL) in collaboration with Sandia National Laboratories. SAM simulates extensive performance and financial information over the lifetime of power plants with renewable energy sources based on system design parameters that are specified as inputs to the model.

Table 2 displays key elements of the cycle design specified in the FOA, and the financial parameters from the SunShot Vision Study (SVS) [2]. These financial parameters were used in the SAM model because they have a direct impact on LCOE, and altering these parameters would not allow for a comparison to previous publications [1-5].

Before work commenced on this development effort, NETL released version 2015.6.30, which included sCO_2 recompression cycles, a feature that was not available when the SunShot Vision Study was performed; thus, it was required to recreate the legacy SVS case in the new version of SAM to ensure that the LCOE matched for similar plant models. The LCOE for these two cases, as shown in Table 3, agree well between the two software versions. Table 3 also shows the LCOE for the SVS inputs when adapted to an sCO_2 cycle type in SAM using the temperature and efficiency targets listed in the APOLLO FOA shown in Table 2. Note that there is a slight increase in the LCOE for this case relative to the original SunShot Study. This increase is likely due to more accurate cost and performance values when modeling an sCO_2 cycle in SAM using the sCO_2 model over the steam model.

Table 2: Key Parameters Used by the SAM Software

Key Parameters Targeted by FOA		Key Financial Parameters from SunShot	
Design HTF inlet temperature (°C)	720	**Inflation rate (%/year)**	3
PHX temperature difference (°C)	15	**Real discount rate (%/year)**	5.5
ITD at design point (°C)	15	**Internal rate of return target**	15 %
Rated cycle conversion efficiency	50%	**IRR maturation (years)**	30
Power block cost ($/kW)	900	**Loan duration (years)**	15
Heliostat field cost ($/m^2)	75	**Loan percent of total capital cost**	60 %
Thermal storage cost ($/kWh$_{th}$)	15	**Loan annual all-in interest rate**	7.1 %

Table 3: Comparison between SAM Versions and Cycle Types for 200 MW CSP Plant

SAM Version	Cycle Type (in SAM)	Cycle Modeled	Real LCOE ¢/kWh	Nominal LCOE¢/kWh
2014.1.14	Supercritical Steam	Supercritical CO_2	6.14	8.42
2015.6.30	Supercritical Steam	Supercritical CO_2	6.16	8.46
2015.6.30	*Supercritical CO_2	Supercritical CO_2	6.45	8.85

*Inputs merged from SunShot Vision Study with new FOA requirements. Note that the cost of the power block in the vision study has decreased from $1200/kWe to $900/kWe.

In addition to verifying the accuracy of the current SAM setup against published data, the system size was optimized to reduce LCE. Results shown in [15] suggest that the optimal system size is between 100-200 MW. This plant configuration would be realized by a number of parallel WRIG Compander units; however, the LCOE with the updated SAM program 2015.06.30 using the aggressive

APOLLO targets was 6.45¢/kWh, falling short of the EERE target of 6¢/kWh.

To further reduce the LCOE of the WRIG Compander plant, the plant's solar multiple was adjusted. The solar multiple scales the heliostat field and receiver size relative to the desired thermal input of the power cycle. Initially, the team selected the same solar multiple as the SVS; however, the system did not appear to be charging the thermal storage enough for sustained operation during winter nights, so the solar multiple was modified to increase the size of the thermal and receiver systems. This increase has an impact on the cost of the system due to increased land, receiver size, and mirrors; however, since more power is produced during the year, the revenue is predicted to outweigh the expense, reducing the LCOE. During the winter, the operation of the cycle extends much further into the night, but during some periods in the summer there is too much solar availability and the system is able to provide energy beyond charging the thermal storage and running the cycle. As a result, the heliostats defocus, which SAM reports as the focus fraction.

One strategy for mitigating this issue is to provide a modular approach to power generation. The compander package can only be scaled to about 25 MW. The studies in SAM assume a 100 MW system, which contains four compander packages. The modular nature of this system allows individual units to be turned on and off in contrast to having a large unit running in part load and having poor efficiency. This means that in the summer, all four units will run, and in the winter only three units are needed.

Previous LCOE studies in this project have utilized the integrated sCO_2 model that is built into SAM. While the SAM cycle model and APOLLO cycle model are similar in off-design trends and magnitudes, they are different enough to affect the LCOE calculation. In order to better match the APOLLO cycle in SAM, the cycle was incorporated into the newest version of SAM (v.2016.03.14) following the previous publication [15]. In the newest version, a user-defined power cycle can be input to allow better customization of how the power cycle behaves. While the custom model provides a tighter control of the cycle input and output behaviour, it still has limitations. Neither the sCO_2 model nor the custom model allows for the precise modulation of the cycle thermal input energy. The APOLLO cycle makes use of inventory control which changes the power cycle mass flow rate, reducing thermal power input. The user-defined model support at NREL indicated that the SAM solver converges on the design thermal energy input, which is fixed at all times unless the turbine output fraction changes. The power output to the grid is only impacted by efficiency changes, not reductions in power cycle mass flow rate, and, according to the APOLLO cycle control scheme, the power out of the cycle when using inventory control should be reduced to 70 MW on extremely hot days. A modification to the SAM code will be required to fully model the impact of inventory control on power produced and energy sold.

Figure 6 presents a rudimentary solution to modeling inventory control in SAM. The monthly averages of ambient temperature were segregated into nine periods. These periods were then input into the thermal storage dispatch schedule. Thus, for each hour of the day of each month, the average thermal reduction due to inventory control is implemented into SAM. Since the temperature varies significantly over a month, this is merely an approximation of how the thermal input should change. However, Figure 6 also shows a much more appropriate trend in power output than previous user-defined model simulations because the power output is affected by time of day. It should be noted that the electric power to grid includes parasitic losses due to pumping molten salt up the power tower. This is why the power produced to the grid is lower during the day than the cycle power output from the Apollo cycle model.

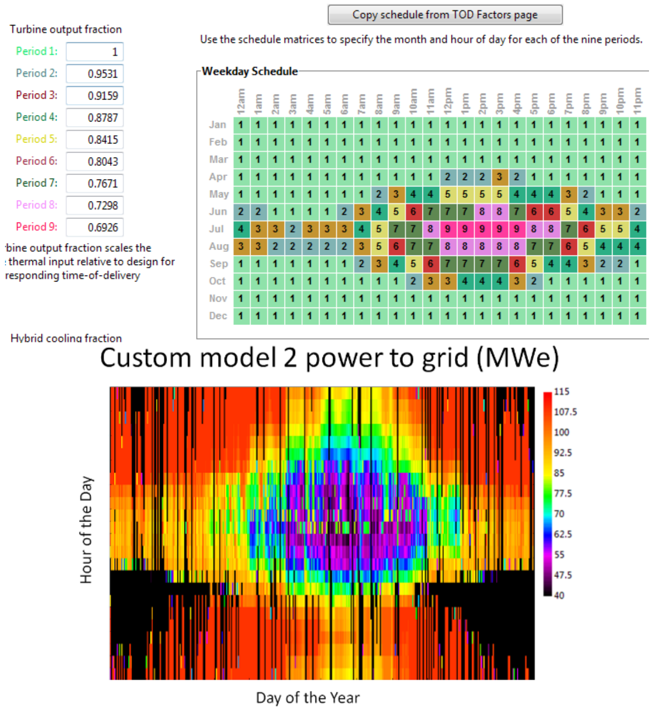

Figure 6: Schedule Changing Heat Input into the Custom Power Cycle Model and Power Produced

The results of all the simulations are given in Table 4. The user-defined model with changing heat input is the closest implementation of the real performance of the Apollo cycle in SAM. All costs of electricity are near the target 6 ₵/kWh. The LCOE of the user-defined cycle is lower than the target, but this is partly because SAM is producing more power than it should on the hottest days.

Table 4: SAM Simulation Results by Model Type

	SAM Default sCO_2 model	SAM default sCO_2 model with modular operation	Apollo-derived user-defined Model	Apollo-derived user-defined model with approximate inventory control
Solar Multiple	3.5	3.1	3.3	3.3
Capacity Factor (%)	66.3	62.6	67.2	65.1
Real LCOE (₵/kWh)	6.16	6.03	5.88	6.16

The user-defined model with approximate inventory control produces a similar LCOE to the default sCO_2 model without modular operation. It is difficult at this time to implement both a modular approach and inventory control into the custom model because they both use the thermal dispatch schedule to tweak SAM thermal inputs. However, once inventory control is supported in SAM, it may be possible to get a similar reduction in LCOE by applying the modular operation scheme to the user-defined model. The default sCO_2 model demonstrates that a modular approach can reduce the LCOE by 2.11%. The user-defined model results do not include a modular operation scheme, but a reduction in LCOE that matches the reduction in the default sCO_2 model will be reflected in the user-defined model results. Thus, an Apollo-derived user-defined cycle model with inventory control and modular operation is estimated to be 6.03 ₵/kWh.

CONCLUSION

This paper presents an interesting concept for a turbomachinery power block that is currently being applied to a supercritical CO2 power cycle for concentrating solar power technologies. This concept utilizes a integrally-geared compander to comprise the turbomachinery on the power block, which has a number of interesting features that are leveraged to improve overall power-block efficiency. The study shows that optimizing thermodynamic efficiency for the given cycle requires the use of a single stage of turbine reheating, which can easily be accommodated into an integrally-geared machine.

Additionally, the authors optimized off-design cycle efficiency at various compressor inlet temperatures by controlling system inventory and compressor IGV angle. The results show a control scheme can that takes advantage of these mass-flow control features to improve off-design efficiency. Note that the off-design efficiency with these features falls short of ideal design-point efficiencies at the various operating temperatures; however, the efficiencies predicted by the current work are well above those that would be attained by a conventional turbomachine without range extension technologies.

These cycle efficiencies were then implemented in a customized SAM model that took advantage of an innovative use of turbine output fraction and explicitly defined system efficiencies to determine LCOE more accurately for the WRIG Compander. Note that even with the range extension features implemented in this development project and state of the art component efficiencies, the LCOE targets were not met without operating multiple units in parallel. This concept improves reliability and improves the system's ability to vary power output to minimize LCOE by increasing runtime while maintaining high efficiency. An estimate of 6.03 ₵/kWh is predicted for the current system.

ACKNOWLEDGMENTS

The team of Southwest Research Institute® (SwRI®) and Hanwha Techwin America, a division of Hanwha Techwin (HTW), were awarded a project funded by the U.S. Department of Energy SunShot Initiative to develop an IGC for use in concentrated solar power (CSP) supercritical carbon dioxide (sCO_2) plant applications. The team thanks the DOE for funding this award DE-EE0007114, and for the guidance of Mark Lawston, Rajagopal Vijaykumar, and Joseph Stekli for helping to manage this award.

REFERENCES

[1] Turchi, C., Mehos, M., Ho, C., & Kolb, G., "Current and Future Costs for Parabolic Trough and Power Tower Systems in the US Market," National Renewable Energy Laboratory, Sandia National Laboratories, Presented at SolarPACES 2010, September 21-24, 2010, Perpignan, France

[2] U.S. Department of Energy, "SunShot Vision Study," February, 2012, DOE/GO-102012-3037, Prepared by National Renewable Energy Laboratory, Accessed 2015, http://www1.eere.energy.gov/solar/pdfs/47927.pdf

[3] Neises, T. and C. Turchi, "Supercritical CO_2 Power Cycles: Design Considerations for Concentrating Solar Power," The 4th International Symposium – Supercritical CO_2 Power Cycles, September 9-10, 2014, Pittsburgh, PA.

[4] Sarkar, J. and S. Bhattacharyya, "Optimization of recompression s-CO_2 power cycle with reheating," Energy Conversion and Management 50, 2009, p. 1939-1945.

[5] Turchi, Craig S., et al. "Thermodynamic study of advanced supercritical carbon dioxide power cycles for concentrating solar power systems." *Journal of Solar Energy Engineering* 135.4 (2013): 041007.

[6] Incropera, F. P., Dewitt, D., Bergman, T., & Lavine, A. Fundamentals of heat and mass transfer. 2007, Hoboken.

[7] Moore, J., & Musgrove G., "Performance and Cost Targets for sCO_2 Heat Exchangers," Panel Session, NETL-EPRI Workshop on Heat Exchangers for Supercritical CO_2 Power Cycles, October 15, 2015, San Diego, CA.

[8] Wilkes, J., Allison, T., Schmitt, J., Bennett, J., Wygant, K., Pelton, R., Bosen, W., 2016, "Application of an Integrally Geared Compander to an SCO2 Recompression Brayton Cycle," Proc. 5th Intl. Symp. – Supercritical CO2 Power Cycles, March 28-31, San Antonio, TX.

[9] Numerical Propulsion System Simulation (NPSS), http://www.swri.org/npss/.

[10] Fact Sheet: Carbon Pricing around the World, Environmental and Energy Study Institute, October 17, 2012, http://www.eesi.org/papers/view/fact-sheet-carbon-pricing-around-the-world?/fact-sheet-carbon-pricing-around-world-17-oct-2012.

[11] NIST REFPROP - http://www.nist.gov/srd/nist23.cfm.

[12] Neises, T. and C. Turchi, "Supercritical CO_2 Power Cycles: Design Considerations for Concentrating Solar Power," The 4th International Symposium – Supercritical CO_2 Power Cycles, September 9-10, 2014, Pittsburgh, PA.

[13] Allison, T., Wilkes, J., Pelton, R., and Wygant, K., 2016, "Conceptual Development of a Wide-Range Compressor Impeller for sCO_2 Applications," *5th Intl. Symposium – Supercritical CO2 Power Cycles*, Short Paper, March 28-31, San Antonio, TX.

[14] Natural Gas Prices: Long Term Forecast to 2020, http://knoema.com/ncszerf/natural-gas-prices-long-term-forecast-to-2020-data-and-charts

[15] 2014, Department of Energy, Office of Energy Efficiency and Renewable Energy, "Concentrating Solar Power: Advanced Projects Offering Low LCOE Opportunities," FOA Number DE-FOA-0001186, CFDA No. 81.087

[16] U.S. Department of Energy, "President Requests $842.1 Million for Fossil Energy Programs," http://energy.gov/fe/articles/president-requests-8421-million-fossil-energy-programs.

[17] EIA Natural Gas Weekly Update http://www.eia.gov/naturalgas/weekly/#tabs-prices-3.

[18] Carbon Dioxide Emissions Coefficients, U.S. Energy Information Administration, 2013, https://www.eia.gov/environment/emissions/co2_vol_mass.cfm.